NEAR-FIELD SCANNING OPTICAL MICROSCOPY (NSOM)

Development and Biophysical Applications

E. BETZIG, A. LEWIS, A. HAROOTUNIAN, M. ISAACSON, AND E. KRATSCHMER
School of Applied and Engineering Physics, and The National Research and Resource Facility for Submicron Structures, Cornell University, Ithaca, New York 14853

ABSTRACT A new method for high-resolution imaging, near-field scanning optical microscopy (NSOM), has been developed. The concepts governing this method are discussed, and the technical challenges encountered in constructing a working NSOM instrument are described. Two distinct methods are presented for the fabrication of well-characterized, highly reproducible, subwavelength apertures. A sample one-dimensional scan is provided and compared to the scanning electron micrograph of a test pattern. From this comparison, a resolution of >1,500 Å (i.e., $\simeq\lambda/3.6$) is determined, which represents a significant step towards our eventual goal of 500 Å resolution. Fluorescence has been observed through apertures smaller than 600 Å and signal-to-noise calculations show that fluorescent imaging should be feasible. The application of such imaging is then discussed in reference to specific biological problems. The NSOM method employs nonionizing visible radiation and can be used in air or aqueous environments for nondestructive visualization of functioning biological systems with a resolution comparable to that of scanning electron microscopy.

INTRODUCTION

Resolving components spatially in biological systems presents a classical biophysical problem. Most imaging techniques presently in use are fundamentally limited by the wavelength of the radiation. In this paper we present our development of a unique new imaging method that is independent of the radiation wavelength. This method permits the nondestructive imaging of surfaces within their native environment, with a resolution comparable to scanning electron microscopy. We have called this advance in biophysical technology "near field scanning optical microscopy" (NSOM).

The resolution limits for this new technique fall between the extremes defined by light microscopy (2,500 Å) and fluorescence energy transfer methods ($\simeq$40 Å to $\simeq$80 Å). Using visible wavelengths, a conservative estimate of the resolution is ~500 Å. Thus, it is likely that this technique will make an important contribution to the investigation of macromolecular assemblies such as lipid microdomains, receptor clusters, and photosynthetic reaction center aggregates. Furthermore, unlike other techniques at this resolution, near-field imaging will be able to follow the temporal evolution of these macromolecular assemblies in living cells. Therefore, NSOM has the potential to provide both kinetic information and high spatial resolution.

Reprint requests should be addressed to Dr. Lewis.

Conceptual Basis of Near Field Scanning Optical Microscopy (NSOM)

The fundamental principle underlying the NSOM concept is outlined in Fig. 1, where visible light is depicted as being normally incident on a conducting screen containing a small (subwavelength) aperture. Because the screen is completely opaque, the radiation emanating through the aperture and into the region beyond the screen is first collimated to the aperture size rather than to the wavelength of the radiation employed. This occurs in the near-field regime. Eventually the effect of diffraction is evidenced as a marked divergence in the radiation, resulting in a pattern that no longer reproduces the geometrical image of the aperture. This occurs in the far-field regime.

To apply the collimation phenomenon, an object, such as a cell membrane, is placed within the near-field region relative to an aperture. In this case, the aperture acts as a light source whose size is not limited by the considerations of geometrical optics. The light source can be scanned over the object, and the detected light can be used to generate a high-resolution image. Because the resolution is dependent upon the aperture size rather than the wavelength, it should be possible to obtain 500 Å or better resolution if a sufficiently small aperture is used. These are the essential features of the NSOM technique, which can be applied in air or aqueous environments using nonionizing, visible radiation. Thus, macromolecular assemblies in functioning biological systems can be imaged at high resolution.

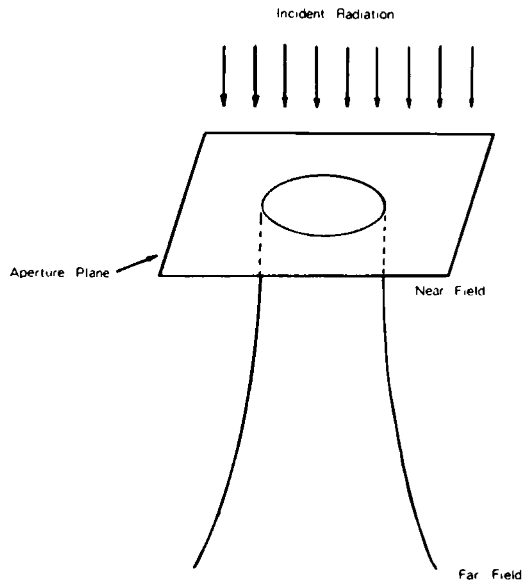

FIGURE 1 Schematic representation showing the collimation of radiation emanating from a subwavelength aperture.

Comparison With Other Optical Methods

It is important to distinguish NSOM from more conventional diffraction limited techniques. For example, although images have been obtained of isolated 250 Å structures using video-enhanced contrast optical microscopy (1), the images of these structures are, in the best of cases, limited by diffraction to sizes of 1,000–2,000 Å. Hence, with this method it is difficult to determine the true sizes of the observed features. Furthermore, two or more structures will not be individually resolved if their respective Airy disks overlap (as determined by the Rayleigh criterion). In comparison, the NSOM method should generate images which indicate the true sizes of assemblies even when these assemblies are separated by much less than the wavelength.

Historical Background

As far back as a decade ago, the principle of super-resolution microscopy was demonstrated at microwave frequencies ($\lambda = 3$ cm) by Ash and Nicholls (2). In their pioneering experiment, a grating of 0.5 mm periodicity was imaged with an effective resolution of $\lambda/60$. However, until we reported our initial results in 1983 (3), there were no published attempts to extend this technique to the visible region of the spectrum. This is quite understandable, because the minute physical dimensions of the optical near-field demand aperture fabrication and micropositioning technologies on a nanometer scale. Furthermore, it is not immediately obvious that the results of the microwave experiment could be extended to the visible regime, because the finite conductivity of thin metal films has to be considered in the design of screens for submicron apertures, whereas the comparatively thicker metal screens used in the microwave case are completely conducting and thus opaque.

Since our original report, several additional publications on near-field imaging technology have appeared (4–11). Fischer (8) has produced an interesting series of results by scanning a subwavelength aperture over a second, larger aperture, but these results are difficult to interpret for a number of reasons. For example, the opacity of the metal films used was not large, so that the apertures were poorly defined and much stray light was transmitted through the aperture screens. In addition, coherent, monochromatic illumination was used at grazing incidence, so that a series of standing waves may have been generated when the polarization of the electric field was perpendicular to these screens.

A near-field imaging system for use in the far infrared is also currently being developed by Massey (10). Although this system may find many applications (such as in the detection of heat transport on a microscopic scale), it will not approach the resolution capabilities of NSOM and can best be viewed as a complementary imaging technique.

Finally, Pohl et al. (11) have developed a system for super-resolution microscopy that shares some of the same features as our NSOM instrument. They call their technique "optical stethoscopy." This is somewhat of a misnomer, as the analogy to a medical stethoscope is not strictly valid. This can be understood by treating the optical aperture and the acoustic stethoscope as classical waveguides. In the optical case, a consideration of the appropriate boundary conditions indicates that all modes are evanescent (decaying) within the aperture (12). Indeed, only the finite thickness of the aperture screen permits the flow of any energy at all. A different set of boundary conditions must be invoked in the acoustic case. These conditions lead to the existence of a single propagating plane wave (13) and explain why a 20 Hz ($\lambda = 17$ m) sonic disturbance can be detected through a long stethoscope tube only a centimeter in diameter.

At the experimental level, the sizes and the structure of the apertures used by Pohl et al. (11) were not characterized. In addition, the nature of their manufacture presents considerable challenges in the attainment of reproducibility. To demonstrate 250 Å resolution using optical techniques, not only must the apertures be well-characterized, but it is also essential to have well-characterized test structures. Neither of these criteria were met in Pohl et al.'s paper.

In short, initial attempts to implement the near-field scanning concept attest to the difficulty of the NSOM technique. To appreciate the technical challenges inherent in this form of microscopy, we have performed model calculations to obtain a first approximation to the pattern of radiation in the near field. These calculations (to be published) investigate the transmission of light through a slit of infinite length in a screen of finite thickness, and were based on the powerful Green's function technique of

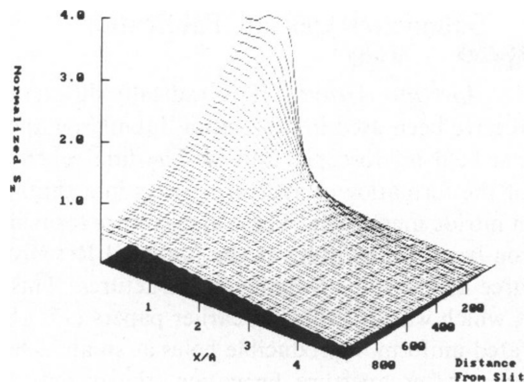

FIGURE 2 The energy flux emanating from a 500 Å wide slit, normalized to the energy of the incident plane wave, is shown plotted as a function of both the perpendicular distance (z) from an 1,800 Å thick conducting screen and the ratio of the lateral distance from the center of the slit to the half width of the slit (x/a). Notice that the radiation is collimated to roughly the edge of the slit ($x/a = 1$) out to $\sim z = 250$ Å.

Neerhoff and Mur (14). In particular, the component of the time-averaged Poynting vector perpendicular to the screen was calculated in the region just beyond the screen. The results are shown in Fig. 2, where the divergence of the energy flux is plotted as a function of the distance from the slit. These results show that the radiation remains collimated to a distance of at least half the slit width. Furthermore, they also indicate that the extent of the near-field increases with the slit width. Finally, these near-field energy flux calculations exhibit a close-to-exponential decrease in intensity with increasing distance from the screen. This suggests that rigid stability requirements will need to be maintained in the z direction, as will be discussed more fully in the following section. Of course, significant differences can be expected between the near-field radiation pattern of a slit and that of a circular aperture, but the simpler slit geometry should give an indication of the pattern to be expected in the aperture case.

TECHNICAL CHALLENGES TO BE ADDRESSED

To construct a super-resolution microscope, several practical considerations must first be addressed. These considerations fall into two broad categories: micropositioning and enhancement of the signal-to-noise ratio.

Micropositioning

The theoretical analysis mentioned above indicates the degree of control required over the aperture-to-object separation. For example, the radiation emanating from a 500 Å-wide slit remains collimated to an approximate distance of 250 Å. Furthermore, because the intensity in the near field is so strongly dependent upon distance, the separation must be maintained with a precision of $\sim$20 Å. To satisfy such strict positioning requirements, several potential problems must be successfully confronted. These are discussed below.

Vibration Isolation. In a typical laboratory environment, building vibrations exist at frequencies as low as 2–4 Hz, although most of the vibrational energy is in the 5–30 Hz range (15). In our environment, we have measured displacements of up to 1 μ in this frequency range. If this energy were to be transferred without attenuation to the critical components of an NSOM system, and if the aperture and object were not held together with sufficient rigidity, then their relative displacement could vary by two to three orders of magnitude greater than the precision required. To preclude this possibility, it is necessary to design an isolation system which attenuates both horizontal and vertical vibrations from the floor at frequencies above a few Hertz. In addition, such a system must use a damping mechanism to insure that any vibrations transmitted to the microscope are transient in nature. This damping mechanism is also needed to reduce the vibrations induced by the motion of the sample stage itself in the course of a scan. Finally, an effective isolation system must also shield the NSOM instrument from acoustic vibrations, which fall in the 20 Hz–20 kHz range.

Thermal Drift. Although the thermal expansion coefficients of the various components of an NSOM system will vary widely with composition and size, it can be expected that these components will expand/contract roughly 0.1–1.0 μm for every 1°C increase/decrease in temperature. Hence, the differential rate of expansion of the aperture relative to an object could present a serious obstacle towards obtaining the required micropositioning capabilities for super-resolution microscopy. This obstacle can be surmounted through two lines of attack: either the instrument can be designed so as to insure that the thermal expansion of the aperture relative to the object is rather small, or else stringent control can be maintained over the temperature of the entire apparatus. Ideally, both of these methods should be used.

Aperture and Sample Translation. As a final micropositioning requirement, it is necessary to translate the aperture and sample accurately relative to one another in all three spatial dimensions. As mentioned above, the translating system should position the aperture with a precision of $\sim$20 Å in the z direction (perpendicular to the sample plane). However, it is equally necessary to obtain accurate positioning in the x and y directions, as one factor which limits the resolution of an NSOM system is the size of the steps taken while scanning. In particular, the step size should be shorter than half of the desired resolution (16). Hence, a system designed for 500 Å resolution must include positioning control of >250 Å in the x and y directions.

Factors Determining the Signal-to-Noise Ratio

Signal Considerations. The light transmitted through a submicron aperture is weak enough to require the use of sensitive detection electronics. A good detection system becomes increasingly important when it is considered that, in the interest of producing high resolution images rapidly, the aperture must scan quickly over the object, so that the time available at each point to accumulate the requisite counting statistics is rather brief. Weak signals can particularly be expected in biological applications, where contrast differences in a specimen can be quite small. In such applications, a variety of nondestructive methods would be needed to increase contrast, ranging from the computer enhancement of images to the fluorescent labeling of specimens.

Noise Considerations. Because rather weak signals are expected, one obvious source of noise is that of statistical noise. The significance of this source can be reduced by increasing the period of data collection, but this is done at the expense of scan speed. Systematic noise can also be expected from the detection system in the form of dark noise and noise from the preamplifier and discriminator electronics. Noise will also be introduced if there is any variation in the light intensity used to illuminate the sample or aperture. Furthermore, because the aperture screen is not completely opaque, any light which is transmitted through this screen (rather than through the aperture) will contribute to the systematic noise.

There are also sources of noise related to the issue of micropositioning. First, unwanted variations in the *xy* positioning of the sample relative to the aperture can either cause an apparent distortion in the image (for variations long compared with the scan time) or else can smear the contrast and resolution information at a point (for variations short compared with the data collection time at that point). Of even more significance are the large variations in apparent signal strength which can be caused by slight changes in the aperture-to-object separation. Finally, noise can be introduced when scanning thick (>1,000 Å), translucent samples, because the system will detect light scattered from the diffraction-limited far-field regions as well as from the collimated near-field regime. In short, considerable effort must be expended to increase signal strength and reduce noise so as to permit rapid high resolution microscopy.

INITIAL FEASIBILITY STUDIES

Our initial goal was to construct a simple prototype to demonstrate the feasibility of the NSOM concept. The essential features of this prototype are discussed below.

Submicron Aperture Fabrication

Aperture Arrays. Two radically different techniques have been used in fabricating submicron apertures for near-field microscopic studies. The first scheme consists of the formation of aperture arrays in a thin, planar silicon nitride membrane. These arrays were formed using electron beam lithography at the National Research and Resource Facility for Submicron Structures. This technique, which was described in earlier papers (17, 18), has generated uniform, reproducible holes as small as 80 Å in diameter. After aperture formation, the opacity of the surrounding membrane was increased by evaporating aluminum over the arrays. Similar apertures have already been applied in optical transmission studies showing that visible light from a tungsten source is transmitted through holes as small as 300 Å (3). The efficiency of the transmission process is shown in Fig. 3 *A*, where light transmission through 2,400 Å-diameter apertures is depicted. Figure 3 *B* demonstrates the alteration in the signal-to-noise ratio in going to a 600 Å diameter aperture array. The uniformity of the transmitted intensity attests to reproducibility

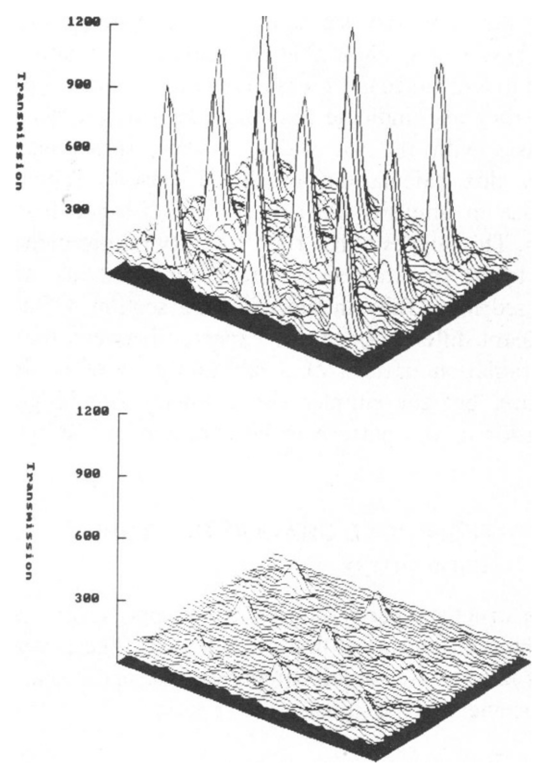

FIGURE 3 (*A*) 5,145 Å light transmission through 2,400 Å diameter apertures is shown detected in the far field with an optical multichannel analyzer. Note the uniformity of the light transmission through the nine apertures shown. Incident beam power was 0.62m W/cm^2. (*B*) 5,145 Å light transmission through 600 Å-diameter apertures is shown as detected in the far field with an optical multichannel analyzer. Incident laser power was as above. Note the even for these smaller apertures a good signal-to-noise ratio is achieved.

of this method of aperture fabrication. In addition to the utility of such arrays in characterizing the optical properties of submicron apertures, they can be applied to non-scanning near-field imaging methods.

Pipette Apertures. The principal problem in near-field imaging is the finite depth of field resulting from the limited extent of the collimation of radiation in the near field. Because of this limitation, apertures in a planar membrane cannot probe recessed regions in rough surfaces. To address this problem, we have developed a simple, inexpensive method of aperture fabrication involving the formation of submicron apertures in the tips of highly tapered, metallized glass pipettes. This method is based on an extension of the technology developed for making glass pipettes used in probing cells electrically by the patch clamp method (19). We have extended this technology by: (*a*) fabricating apertures with diameters of <1,000 Å; (*b*) characterizing the apertures at the tips of the pipettes with scanning electron microscopy; (*c*) showing that light is transmitted through such pipette apertures.

A two-stage method was used for constructing the apertures. The first stage tapered the pipette and the second stage pulled until the breaking point was reached. By varying the wall thickness of the glass pipettes, aperture diameters from <1,000 Å–5,000 Å with outer diameters of 5,000 Å–7,500 Å were reproducibly generated. Thicker-walled pipettes were found to produce smaller apertures.

FIGURE 4 A scanning electron micrograph of the tip of a metallized pipette is shown with a 5,000 Å outer diameter and with a <1,000 Å central aperture. Although even smaller apertures could be prepared with our technique, they would be difficult to characterize with the limited resolution of the SEM available.

Aluminum was again evaporated to increase the opacity of the glass wall surrounding the aperture. This evaporation resulted in a uniformly metallized tapered pipette with an aperture <1,000 Å at the tip (see Fig. 4).

The taper of the pipette is of particular importance. When light is passed down the pipette, it is transmitted through the outer glass walls as well as through the central region (see Fig. 5). The inner diameter of the pipette rapidly tapers to dimensions of less than an optical wavelength. This model of light transmission suggests that the radiation exists in a propagating mode throughout the length of the pipette, since the pipette outer diameter is larger than the cut-off value calculated by treating it as a classical wave guide. Only at the thin metallized region at the tip of the pipette is the cut-off threshold reached. Thus, the large throughputs observed are a consequence of the fact that the region of evanescence is short. After leaving the aperture, the radiation once again exists in a propagating mode.

An NSOM Prototype—Design

The pipette-type apertures were an important advance in our development of a simple NSOM prototype, but even for the initial feasibility experiments, the technical challenges discussed above had to be addressed in at least a preliminary fashion. The consideration of these challenges in our development of a workable NSOM prototype will now be discussed.

Initial System. A two-stage system was used to shield the instrument from floor vibrations. The first consisted of a large table top mounted on tennis balls. Measurements in our laboratory indicated that this system reduced high frequency vertical disturbances to amplitudes of <300 Å. The second consisted of a heavy steel plate resting on a foam pad, which provided isolation in the intermediate frequency range (10–50 Hz).

Using precision translation stages and conventional micrometers, the pipette was positioned with ~1 μm accuracy in the *xy* plane over the section of the sample to be

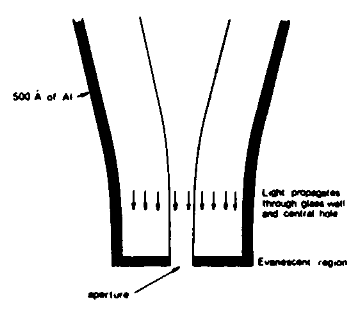

FIGURE 5 A cross-sectional representation of a metallized pipette is shown together with the propagation of light toward the tip.

scanned. Another stage was used to position the pipette within a few microns of the sample surface. To bring the pipette within the near-field region, a stacked piezoelectric element was used (see Fig. 6). A low-noise (15 mV peak to peak), high-voltage supply was used to insure that the error in the piezoelectric expansion due to voltage ripple was considerably less than the 20 Å limit mentioned previously. Another piezoelectric element was used to drive the pipette in the scan direction. The step size could be varied, but was typically 150 Å. Because conventional piezoelectric elements have limited expansion ranges, the scans were constrained to be no larger than several μm. Furthermore, these conventional elements exhibit hysteresis problems ($\simeq$15% of the full expansion), so that accurate positioning could be achieved only along a single axis.

To deal with the problems posed by signal-to-noise considerations, the prototype system (see Fig. 6) used an optical multichannel analyzer with an SIT vidicon detection system in conjunction with a conventional light microscope. This design insured that a sufficient portion of the available light was collected and detected. Noise in each channel of the detector was at most half the signal due to the aperture, even when small apertures and weak (tungsten) illumination were used. Much of the noise consisted of a constant background level, which was easily subtracted. To measure the noise from other sources, the final detection signal was plotted as a function of time in a test situation where the aperture position was fixed. The resulting variations in intensity were roughly one percent of the apparent signal. These noise fluctuations were at least an order of magnitude smaller than the intensity changes observed in the course of a super-resolution scan.

NSOM Prototype—Results

Microfabricated Patterns for Resolution Tests. To test the NSOM method, it was necessary to fabricate objects that could be used to define the resolution limits of the resulting device accurately. Toward this end, electron beam lithography was used to create a mask consisting of several sets of line gratings with varying periodicity. The image of this mask was reproduced with high fidelity as a series of aluminum lines on a glass coverslip using the method of contact printing. These lines were 2,000 Å wide and were separated by spacings ranging from 2,000 Å–8,000 Å. In Fig. 7, a scanning electron micrograph of one of these gratings is shown. Note the quality with which the pattern is reproduced. As noted above, such high-quality test objects with reproducible features are required before any conclusions can be drawn about NSOM resolution.

A One-Dimensional Scan. Using the NSOM prototype and the test object discussed above, a one-dimensional scan was performed that demonstrated super-resolution capabilities. The light from a 100W tung-

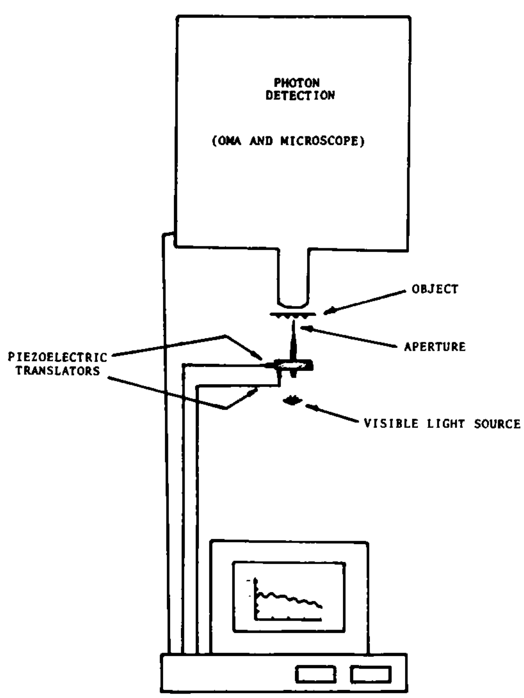

FIGURE 6 A schematic diagram of the experimental apparatus used for our initial feasibility experiments is shown. Both the optical multichannel analyzer and the piezoelectric translators are controlled with a microcomputer.

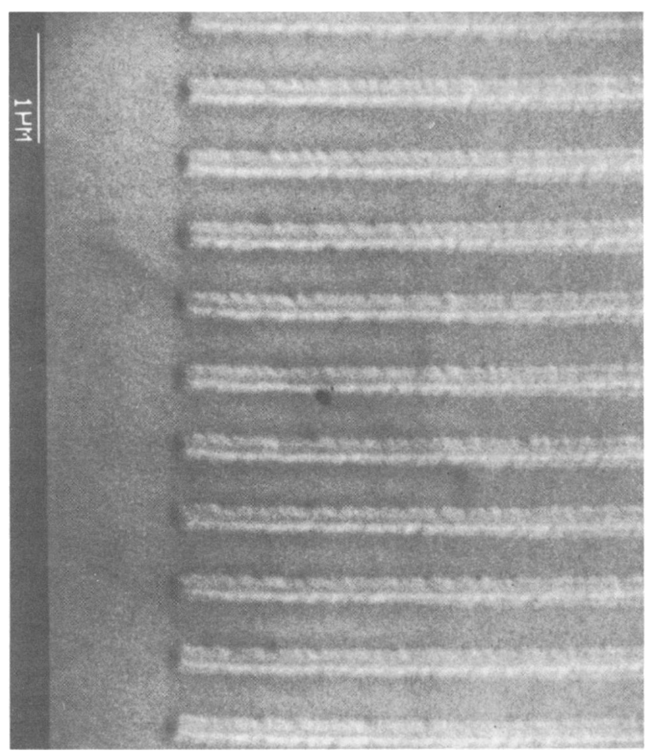

FIGURE 7 A scanning electron micrograph of a grating of aluminum lines on glass used for our resolution tests is shown. The lines were 2,000 Å separated by 4,000 Å. To obtain this micrograph the sample was coated with a 100 Å thick film of gold palladium.

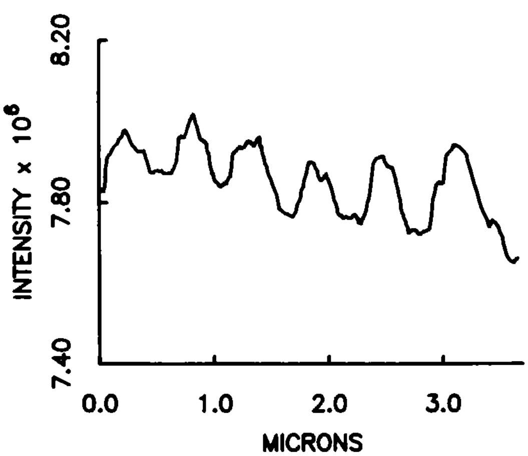

FIGURE 8 A scan of the test grating in Fig. 7 is shown. From the sharpness of the intensity modulation between adjacent maxima and minima, a resolution of <1,500 Å is inferred. Furthermore, note that the periodicity of the grating is reproduced over the entire scan.

sten lamp was passed through a pipette to illuminate the aperture. The tip was brought into contact with the sample surface and then was retracted several nanometers for scanning.

The initial scan was performed using a 5,000 Å diameter pipette-type aperture; the results are shown in Fig. 8. Note that the periodicity of the grating pictured in Fig. 7 is reproduced throughout the entire length of the NSOM scan. A resolution of >1,500 Å is inferred from averaging the sharpness of the steps in going from transmission minima to adjacent transmission maxima and vice versa. Note further that the technique permits detection of sharp edges with a resolution considerably better than the limit expected based on a naive model of the aperture size. This is understandable, because with a sufficient signal-to-noise ratio it should be possible to detect changes in intensity due to partial occlusion of the aperture by the sharp edge.

Future Improvements

Although the prototype system was sufficient to demonstrate the super-resolution concept, it suffered from a number of limitations. These included the inability to scan in two dimensions, the inability to scan over rough topography, the inability to produce highly reproducible scans, and the inability to scan at high speed. Methods exist for attacking all these problems. We are currently incorporating these methods in the construction of a second-generation NSOM instrument. Many of the ideas used in this construction effort were first developed for scanning tun-

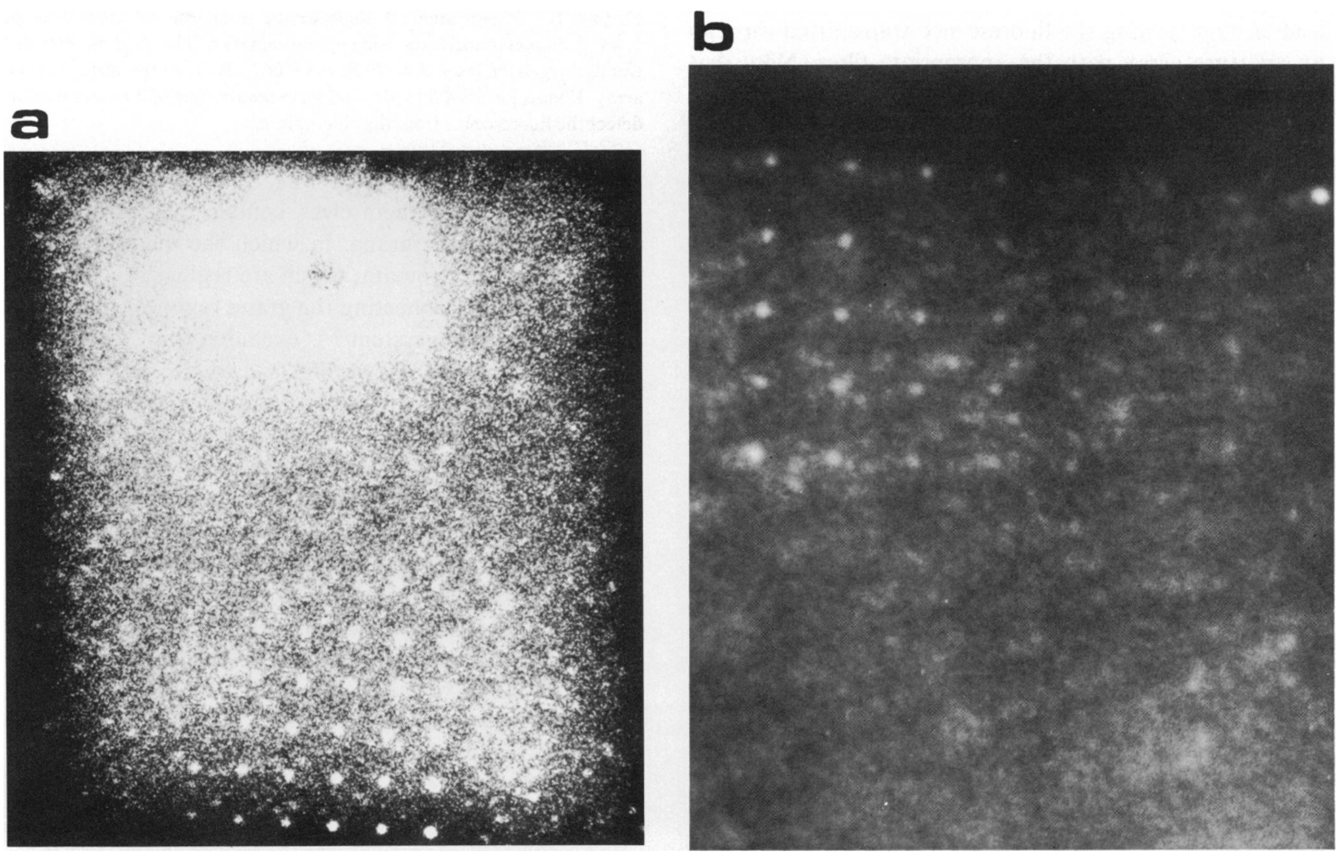

FIGURE 9 Perylene fluorescence through (*a*) 1,200 Å diameter and (*b*) 600 Å diameter apertues are shown. The exciting laser light at 5,145 Å illuminated the sample from below, and the fluorescence was detected through the apertures from above. The laser power that was used caused no detectable bleaching of the sample. The fluorescence was recorded with ASA 400 Kodak Ektachrome film using a 30 s exposure. These arrays contain graduated aperture sizes with the maximum corresponding to the diameters noted above. Please refer to the color figure section at the end of this book.

neling microscopy, where positioning on a subangstrom scale is required (20). At the completion of this effort, we hope to have a versatile system capable of investigating problems of biophysical interest.

BIOPHYSICAL APPLICATION

Fluorescence Detection

Because NSOM uses visible radiation, many of the techniques already developed for conventional microscopy (e.g., polarized illumination, phase contrast methods, etc.) can be used to advance the biophysical applicability of super-resolution microscopy. In particular, contrast enhancement by fluorescence techniques will be useful, because many biological systems can be selectively and nondestructively labeled with fluorophores; others contain fluorescent domains in their natural state. The only potential problem associated with fluorescent labeling lies in the reduction of the signal strength because of the limited cross-sections and quantum yields of these fluorophores. However, in this paper, we have taken a first step in demonstrating the feasibility of fluorescence imaging by observing fluorescence emanating from subwavelength apertures (see Fig. 9). This result was obtained by illuminating a thin film of perylene with 5,145 Å radiation from a laser, and viewing the fluorescence transmitted through an aperture array with the appropriate filter. Note that relatively strong signals are obtained, even though perylene has only a moderate quantum efficiency.

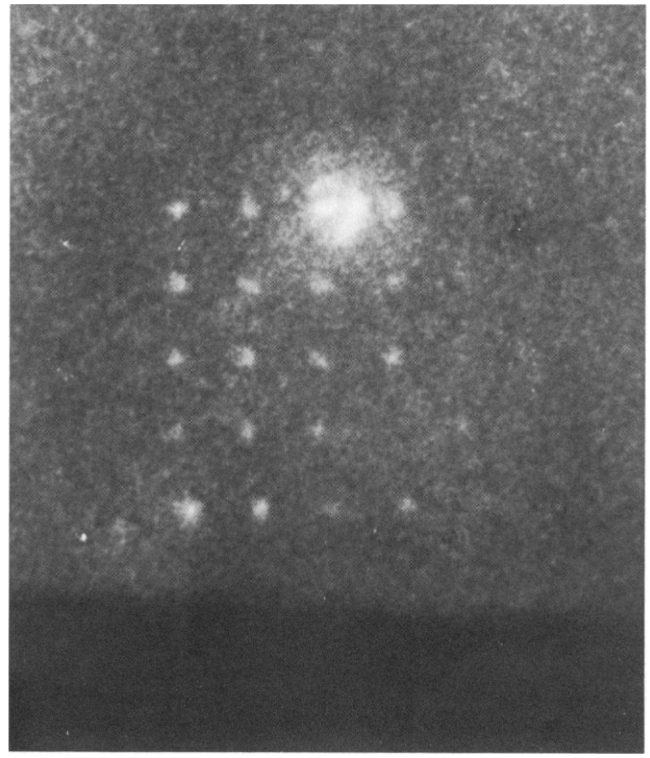

FIGURE 10 Photosystem II fluorescence is shown detected through 2,400 Å diameter apertures using epi-illumination. The incident intensity from an argon ion laser at 4,579 Å was 0.067 $\mu W/\mu^2$ at the surface of the array. Kodacolor ASA 400 film and an exposure time of 40 s was used to detect the fluorescence from the chloroplasts.

Fluorescence From a Functioning Biological System

The next step in approaching a significant biological problem involved observing the transmission of fluorescent light through submicron apertures emanating from a viable biological specimen. To acheive this, spinach chloroplasts were used. A suspension of such chloroplasts was placed directly on an array of 2,400 Å holes, and the suspension was made sufficiently dense so that the chloroplasts adhered to the array and did not migrate. The chloroplasts were illuminated through the apertures using 4,579 Å laser radiation incident from the opposite side of the array, and the fluorescence was detected back through these same apertures in reflection. The results, shown in Fig. 10, demonstrate the feasibility of detecting such fluorescence on a submicron scale in a nondestructive manner.

Chloroplasts were chosen for our initial experiments because they are involved in the current debate concerning the distribution of the two photosystems involved in photosynthesis. Photosystem II is involved with the splitting of water while photosystem I is involved with the alteration in the oxidation-reduction potential of electrons ejected from the split water. Both photosystems are found in the thylakoid membranes of chloroplasts, but only photosystem II fluoresces at room temperature.

The membranes themselves contain two structurally distinct regions: the grana, in which the membranes are stacked; and the stromata, which are regions of unstacked membranes interconnecting the grana regimes. According to one model, photosystem I is excluded from the stacked regions of the grana. However, the evidence on which this model is based comes from freeze-fracture electron microscopy, detergent methods of fractionating the grana and stroma membranes, and mechanical fractionating methods (21, 22), all of which have a disruptive effect on the membranes. Conventional microscopy cannot be used because the grana regions cannot be resolved with sufficient clarity to determine the distribution of the two photosystems. In contrast, near-field microscopy should provide the resolution necessary to determine the photosystem distribution within viable chloroplasts maintained in their native environment. We are currently working on this problem. Our results should help elucidate energy transfer mechanisms involved in photosynthesis.

Signal-to-Noise Ratio Calculations for Biological Applications

The signals detected by fluorescence NSOM imaging are weak and many possible sources of noise can be expected. In this section we illustrate the feasibility of fluorescence imaging methods by calculating the signal-to-noise ratio in a specific biological application. The particular problem we focus on is the detection of a receptor in the plasma membrane of human fibroblast cells that binds low density lipoprotein (LDL). LDL is the predominant transporter of plasma cholesterol, and at least 30 fluorescent lipid molecules can be incorporated per LDL molecule (23). It has been shown that with the fluorescent lipid 3, 3′-dioctadecylindocarbocyanine iodide (diI[3]), single LDL molecules on single LDL receptors can be detected (23). We can use this data to obtain signal-to-noise estimates that will indicate the feasibility of imaging such receptors. However, these calculations are not limited to this example, because phycobiliproteins have been shown to be as highly fluorescent as LDL and can be used to label selectively a variety of cellular receptors (24). We have been able to irradiate LDL molecules with green light for ~1 min at an intensity of 1 $\mu W/\mu^2$ before the resulting fluorescent image begins to fade. This corresponds to a total dose of 1.9×10^{22} photons/cm^2.

To determine how this limit affects the incident intensity and hence the total signal in an NSOM application, we consider here the specific case of near-field microscopy in reflection. The use of such a geometry is advantageous, because each molecule is affected only when the illuminated aperture is overhead. In practice, this is not strictly true, because the finite opacity of the screen must be taken into account. For example, a 600 Å-thick layer of aluminum will transmit ~0.01% of the incident light. If the attenuation of the radiation in the aperture is assumed to be 90%, then the differential transmittability of the aperture relative to the screen is 10^3.

In a typical scan, we may wish to record a 100×100 element image within 100 s. In this case, the differential transmittability indicates that the LDL molecules will receive dosages roughly ten times greater from transmission through the screen as they will from transmission through the aperture. Hence, to remain below the photobleaching threshold within the 100 s scan time, a maximum photon flux past the screen of 1.7×10^{20} photon/s/cm^2 is permissible, corresponding to an incident intensity of 5.4 mW/μ^2.

Although at first glance it may appear troubling that the dosage from screen transmission is an order of magnitude greater than that from aperture transmission, when the situation is considered in detail it is not problematical at all. First, it must be remembered that these figures refer to the total dosages in the course of a scan, and at any given time the intensity directly below the aperture is ~1,000 times greater than the intensity below the screen. Furthermore, from the standpoint of the signal-to-noise ratio, we are only interested in the fluorescent light that is transmitted back through the aperture and screen for eventual detection. In as much as this is the case, the transmission of light through the screen is unimportant, because any fluorescence which might otherwise be generated by LDL molecules under the screen is highly quenched by the presence of the metal within the screen (25). Hence, only the fluorescence from the near field directly below the aperture contributes to the signal, and only far-field fluorescence contributes to the noise.

The maximum permissible intensity calculated above can now be used to estimate the total signal which can be expected in our Gedanken experiment. In particular, by again assuming a 10% transmitability for the aperture and noting that the above scan parameters lead to a 10 ms exposure time per pixel location, we find that 1.7×10^{21} photons/cm^2 for each pixel are transmitted through the aperture. We will further assume that these photons are all incident on the fluorescent site of a single receptor.

To calculate the resulting signal, we note that each of the 30 diI chromophores per LDL molecule has an effective photoabsorption cross section of 3.8×10^{-17} cm^2 with a fluorescent yield of 0.1 (23). Using these numbers we find an initial signal of 1.9×10^5 fluorescent photons/pixel.

A number of factors cause the detected signal to be lower than this initial value. First, in the reflection mode described here, the assumed aperture transmission reduces the fluorescent light intensity by 90%. Second, inefficiencies in the collection optics can be assumed to reduce the intensity further by 50%. Finally, the photomultiplier that will form the heart of a sensitive detection system has a quantum efficiency of only 20%. When all these factors are taken into account, the detected signal is found to be 1.9×10^3 counts/pixel.

To determine the noise associated with a signal of this strength, we first consider noise due to photon counting. Statistical noise for the above counting level is ~44 counts/pixel. In contrast, dark noise from the photomultiplier should be <10 counts/s. For the above scan rates, this corresponds to 0.1 counts/pixel, and hence is quite negligible.

Other fundamental sources of noise arise from the limited extent of the collimation of radiation in the near field. For example, although the LDL molecules in close proximity to the metal screen will not exhibit fluorescence, other such molecules bound to the far side of the cell membrane will be weakly illuminated by residual far-field radiation from the aperture, and hence may yield dim fluorescence noise. This noise is considerably less than the signal due to fluorescence from receptors within the intense near-field radiation pattern emanating from the aperture, as can be understood by the following simple argument.

As was mentioned previously, the intensity of radiation emanating from a slit falls in an almost exponential manner within the near field. It is reasonable to assume that similar behavior exists in the case of a circular aperture. In fact, by treating an aperture of diameter d = 500Å as a waveguide, a specific form of $\exp[-2\pi r/d]$ can be assumed to hold out to a collimation distance of ~250 Å. Hence, the radiation should remain collimated through the entire thickness of that portion of the cell membrane which is directly under the aperture, and any fluorescence that occurs in this region can be considered to contribute to the signal. In contrast, any fluorescence which occurs in the far-field region contributes to the noise. However, within the far field, the aperture can be modeled as a dipole radiator, so that the outward flux falls as $1/r^6$. If we assume that this behavior is valid up to $r = 250$ Å, then the continuity of intensity at this distance can be used to provide a complete, qualitiative model of the energy flow past the aperture.

We can now use such a model to estimate the signal-to-noise ratio caused by the limited extent of the collimated near field. The signal is determined by integrating the exponential intensity factor over a hemisphere of 250 Å radius. Similarly, by integrating the factor of $1/r^6$ over a 250 Å-thick shell 1 μm away (which represents the membrane furthest from the aperture), the noise is found. In this example, which should fairly well model the binding of LDL receptors to fibroblast cells, the noise is found to be several orders of magnitude less than the signal. Even if we were to assume that chromophores are evenly distributed throughout the bulk of the cells (certainly not the case in our example), a signal-to-noise ratio of 7.7 can be obtained using this model. When it is also considered that the fluorescence from the chromophores decreases in intensity by $1/r^6$ as well, the noise is dropped even further.

The implications of this last point cannot be overemphasized. The finite extent of the near-field is used to advantage since the far-field noise is small compared with the near-field signal. Thus, NSOM can be used to image surfaces on thick samples without sectioning.

Returning to our model for imaging LDL receptors, it can now be seen that the most significant source of noise is statistical in nature. Thus, by using the above results, we find that a signal-to-noise ratio of ~44 should be obtainable, and hence the experiment should be entirely feasible. Indeed, it would not be necessary to run the experiment at the threshold for photobleaching. If, for example, the incident intensity were to be decreased by a factor of ten, a signal-to-noise ratio of almost 14 would still be achieved. Alternatively, the size of the scan speed could be increased by a factor of ten with an identical change in the signal-to-noise ratio.

CONCLUSIONS

Our initial prototype system has demonstrated the feasibility of NSOM as a high-resolution imaging technique. Furthermore, the results of the fluorescence experiments and the signal-to-noise ratio calculations indicate that NSOM may be applied to a variety of biological problems. For example, with the development of a flexible second generation system, NSOM could be used to: image lipid microdomains in model membrane assemblies (26) or living cells; investigate banding patterns in chromosomes with fluorescent molecules that bind to particular DNA sequences and structures (27); delineate cystoskeletal interactions with membrane bound proteins; characterize alterations in cell surface topography as a result of cellular stimulation (28); visualize organelle movement along dissociated actin filaments (29); and study the kinetics of specific proteins during muscle contraction (30). In addition, this technique could be used to investigate problems in many other areas from microelectronics to chemistry where nondestructive, high-resolution imaging is required.

The chloroplast imaging experiments are in collaboration with Prof. Chanoch Carmeli. We would like to thank Brian Whitehead for electron beam exposure of the mask gratings.

This work is supported by U.S. Air Force contract 84-NE-121 and the National Research and Resource Facility for Submicron Structures through National Science Foundation contract EC58200312. Support from the U.S. Army in the initial phases of this research was provided to A. Lewis through contract DAMD17-79-C-9041.

Received for publication 11 May 1985 and in revised form 1 July 1985.

REFERENCES

1. Allen, R. D. 1985. New observations on cell architecture and dynamics of video-enhanced contrast optical microscopy. *Annu. Rev. Biophys. Chem.* 14:265.
2. Ash, E. A., and G. Nicholls. 1972. Super-resolution aperture scanning microscope. *Nature (Lond.)*. 237:510.
3. Lewis, A., M. Isaacson, A. Muray, and A. Harootunian. 1983. Scanning optical microscopy with 500 Å spatial resolution. *Biophys. J.* 41(2, Pt.2):405*a*. (Abstr.)
4. Lewis, A., M. Isaacson, A. Harootunian, and A. Muray. 1984. Development of a 500 Å spatial resolution light microscope. *Ultramicroscopy*. 13:227.
5. Harootunian, A., E. Betzig, A. Muray, A. Lewis, and M. Isaacson. 1984. Near field investigation of submicrometer apertures at optical wavelengths. *J. Opt. Soc. Amer.* A1:1293.
6. Betzig, E., A. Harootunian, A. Lewis, and M. Isaacson. 1985. Near field scanning optical microscopy (NSOM). *Biophys. J.* 47(2, Pt.2):407*a*. (Abstr.)
7. Betzig, E., A. Harootunian, E. Kratschmer, A. Lewis, and M. Isaacson. 1985. Nondestructive optical imaging of surfaces with 500 Å resolution. *Bull. Amer. Phys. Soc.* 30:482.
8. Fischer, U. Ch. 1985. Optical characteristics of 0.1 μm circular apertures in a metal film as light sources for scanning ultramicroscopy. *J. Vac. Sci. Technol.* B.3:386.
9. Massey, G. A. 1984. Microscopy and pattern generation with scanned evanescent waves. *Appl. Opt.* 23:658.
10. Massey, G. A., J. A. Davis, S. M. Katnik, and E. Omon. 1985. Subwavelength resolution far-infrared microscopy. *Appl. Opt.* 29:1498.
11. Pohl, D. W., W. Denk, and M. Lanz. 1984. Optical stethescopy: image recording with resolution $\lambda/20$. *Appl. Phys. Lett.* 44:652.
12. Jackson, J. D. 1978. Classical Electrodynamics. 2nd ed. John Wiley and Sons, New York. 344.
13. Kinsler, L. E., A. R. Frey, A. B. Coppens, and J. V. Sanders. 1982. Fundamentals of Acoustics. 3rd ed. John Wiley and Sons, New York. 218.
14. Neerhoff, F. L., and G. Mur. 1973. Diffraction by a slit in a thick screen. *Appl. Scient. Res.* 28:73.
15. Newport Research Corporation Catalog. 1983–84. Vol. 13 Fountain Valley, Ca.
16. Shannon, C. E. 1949. Communication in the presence of noise. *Proc. IRE.* 37:10.
17. Muray, A., M. Isaacson, I. Adesida, and B. Whitehead. 1983. Fabrication of apertures slots and groves at the 8–80 nm scale in silicon and metal films. *J. Vac. Sci. Tech.* B1:1091.
18. Isaacson, M., A. Muray, M. Scheinfein, I. Adesida, and E.

Kratschmer. 1985. Nanometer structure fabrication using electron beam lithography. *In* Proceedings of the International Symposium on Nanometer Structure Electronics, Osaka. K. Gamo, editor. Ohmsha, Ltd., Tokyo.
19. Single Channel Recording. 1983. B. Sakmann and E. Neher, editors. Plenum Press, New York.
20. Binnig, G., and H. Rohner. 1982. Scanning tunneling microscopy. *Helvetica Physica Acta.* 55:726.
21. Anderson, J. M. 1981. Consequences of spatial separation of photosystem 1 and 2 in thylakoid membranes of higher plant chloroplasts. *FEBS* (*Fed. Eur. Biochem. Soc.*) *Lett.* 124:1.
22. Barber, J. 1980. An explanation for the relationship between salt-induced thylakoid stacking and the chlorophyll fluorescence changes associated with changes in spillover of energy from photosystem II to photosystem I. *FEBS* (*Fed. Eur. Biochem. Soc.*) *Lett.* 118:1.
23. Barak, L. S., and W. W. Webb. 1981. Fluorescent low density lipoprotein for observation of dynamics of individual receptor complexes on cultured human fibroblasts. *J. Cell Biol.* 90:595.
24. Oi, V. T., A. N. Glazer, and L. Stryer. 1982. Fluorescent phycobiliprotein conjugates for analyses of cells and molecules. *J. Cell Biol.* 93:981.
25. Drexhage, K. H. 1974. Interaction of light with monomolecular dye layers. *Progr. Opt.* 12:165.
26. Hui, S. W., and D. F. Parsons. 1975. Direct-observation of domains in wet lipid bilayers. *Science* (*Wash. DC*). 190:383–384.
27. Barton, J. K., L. A. Basiles, A. Banishefsky, and A. Alexandrescu. 1984. Chiral probes for the handedness of DNA helixes: enantiomers of tris (4, 7-diphenylpheanthroline) ruthenium (II). *Proc. Natl. Acad. Sci. USA.* 81:7.
28. Fernandez, J. M., E. Neher, and B. D. Gomperts. 1984. Capacitance measurements reveal stepwise fusion events in degranulating mast cells. *Nature* (*Lond.*). 312:453.
29. Kachar, B. 1985. Direct visualization of organelle movement along actin filaments dissociated from Characean algae. *Science* (*Wash, DC*). 227:1355.
30. Somlyo, A. P., and A. V. Somlyo. 1985. Smooth muscle structure and function. *In* Handbook of Experimental Cardiology. H. M. Fozzard, E. Haber, R. B. Jennings, A. M. Katz, and -H E. Morgan, editors. Raven Press, New York. In press.

DISCUSSION

Session Chairman: Benno Schoenborn
Scribes: Robert V. McDaniel and Dinakar Salunke

WARE: Does the transmission of the aperture depend on the shape of the wavefront or on the wavelength?

BETZIG: The transmission of a small aperture in the near field depends on the area of the aperture for both an incident plane wave and an incident converging wavefront. Transmission drops as the fourth power of the wavelength and increases as the fourth power of the aperture radius.

STEWART: I would like to ask a couple of technical questions. What is the depth of focus for NSOM? Would there be light scattering problems due to passage of the light from the aperture through the cell before it reaches the detector, which may affect your resolution?

BETZIG: The depth of field is quite small. For example, it is 200 Å for a 500-Å diameter aperture. Because of the narrow depth of field, we must use a feedback system to maintain the distance from the aperture to the specimen. For example, the methods of scanning tunneling microscopy or capacitance microscopy could be used. One could also monitor the fluorescence of a uniformly distributed fluorophore and use the variations of intensity in the near field to monitor the distance. With regard to scattering by the cell, this is a signal-to-noise problem. The light from the surface is the signal and the scattered light can be considered to be noise. This technique is solely a surface probe; the interior of cells cannot be studied. We can also use either reflected light or reflected fluorescence (epi-illumination) to avoid scattering by the interior of a thick specimen.

STEWART: Let me understand this correctly. Is there indeed a rapid falloff of the signal with distance from the aperture?

LEWIS: Yes, because of the exponential decrease in the near-field intensity. Also, for fluorophores out of the near-field, there is a $1/r^6$ dependence in the fluorescence, so that only fluorophores near the aperture contribute to the signal.

STEWART: So therefore the method would be useful mainly for examining the cell surface?

BETZIG: Yes. There is also the possibility of doing reflection microscopy, in which the near-field phenomenon is used both coming and going. Then the aperture is used to illuminate only a small section of the surface, and the light is collected from only the same small area. The resolution of the reflection technique is probably better than from transmission, but the signal-to-noise ratio will be decreased by the light having to pass twice through the aperture.

STEWART: In the periodic scan that you have shown, what was the spacing of the lines? Have you used Fourier transform techniques to look for higher orders?

BETZIG: We have not done that with our scans, but we have done this with super-resolution lithography of the test pattern. We observe three orders and the spacing is 2,000 Å.